A 2-ft length of X-band waveguide (WR-90) was measured by this method and a dissipative loss of 0.12 ± 0.02 dB was found at 8700 MHz. If the correction for the short cavity had been neglected, the apparent loss would have been 0.18 dB. The irises were made from 0.020-in copper by punching 3/16-in diameter holes.

Conclusions

Since the losses of both irises and the launching and receiving sections are all lumped together, the correction for these losses is approximate. However, the waveguide-attenuation measurement is practical only when these losses are small enough so that the approximation introduces negligible error. At the same time, these losses are often too large to be neglected entirely.

The curve-fitting algorithm that has been described is capable of determining the Q of microwave circuits with as much accuracy and reproducibility as can be hoped for in dealing with practical circuits. The reproducibility of connections is generally the limiting factor in circuits of the type studies. (Special cavities could be designed as Q standards for more critical evaluation of reproducibility and for intercomparison of different instruments and methods.)

The algorithm has a modest ability to find and converge upon a resonance, if given a good initial guess, which is usually a simple matter in production testing of similar parts.

However, the search capability could be enhanced by using the measured transmission magnitude as a weighting factor. This technique would increase the computation required but would make better use of the measurements.

Acknowledgment

The author wishes to thank Computer Metrics, Inc., Rochelle Park, N.J., and Palo Alto, Calif., for making the automatic network analyzer time available.

References

[1] C. G. Montgomery, R. H. Dicke, and E. M. Purcell, *Principles of Microwave Circuits*. New York: McGraw-Hill, 1947.

Impedance Measurements of Microwave Lumped Elements from 1 to 12 GHz

ROBERT E. DeBRECHT, MEMBER, IEEE

Abstract—**The impedance measurement of small, microwave lumped elements of the order of 1 mm has been extended up to 12 GHz by a technique in which the frequency and Q of a resonant transmission line are perturbed by the connection of a lumped element. With the use of low-loss resonant coaxial lines, the technique has been applied to the measurement of lumped-element capacitors ranging from 0.4 to 3.6 pF and inductors ranging from 1.1 to 4.3 nH. Conductor Q values for capacitors as high as 1700 at 1.4 GHz and 100 at 12 GHz have been measured and estimates of dielectric Q values for capacitors of over 5000 have been obtained. Single-turn 1.1-nH inductor Q's of 40 at 1 GHz and 90 at 7 GHz have also been measured. The capacitors and single-turn inductors are found to have constant C and L values up to 12 GHz.**

Manuscript received March 4, 1971; revised September 9, 1971. The work in this paper was supported by the U.S. Army Electronics Command, Fort Monmouth, N. J., under Contract DAAB07-68-0296, and by RCA Laboratories, Princeton, N. J.

The author is with RCA Laboratories, Princeton, N. J. 08540.

I. Introduction

AT MICROWAVE frequencies the increasing use of solid-state active devices and the trend toward smaller electronic packages has stimulated an interest in replacing distributed circuits with smaller sized lumped-element circuits. In the past the use of lumped elements has been limited in frequency to below 1 GHz by problems of fabrication and relatively high losses. However, because of recent advancements in the technology of thin-film fabrication [1], [2], low-loss lumped-element circuits capable of competing with distributed circuits have been made in the S- and C-band ranges [1]–[6]. Unfortunately, the losses of lumped elements operating in the gigahertz range have been difficult to measure. The smaller sizes and lower

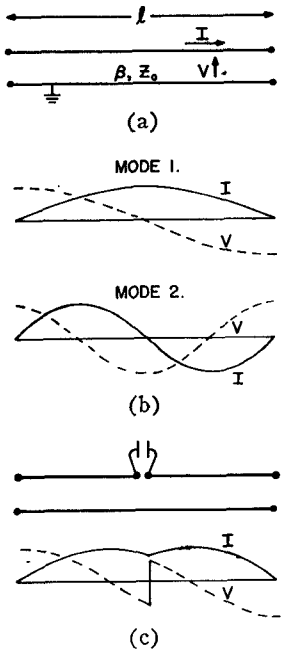

Fig. 1. (a) Schematic representation of a transmission line. (b) The standing waves for two modes of resonance. (c) Series connection of a capacitor and the resulting standing-wave pattern.

resistances of the elements, and problems arising from radiation have placed frequency limitations on conventional measurement techniques. The commonly used technique, a slotted-line measurement, is limited to below 3 GHz by measurement accuracy and the magnitude of the corrections that must be made to the measured data [7].

This paper describes a resonance measurement technique capable of measuring the loss of the high-frequency lumped elements. The application of the technique to the measurement of lumped-element inductors and capacitors from 1 to 12 GHz and the results of the measurements are presented.

II. Theoretical Considerations

The technique developed here for the measurement of lumped-element impedance values makes use of the frequency and Q of a resonant transmission line. By connecting a lumped element to the line, the frequency of resonance and Q are perturbed; and from the perturbations, the impedance of the element can be found. Since the transmission line resonates at multiples of some basic frequency, the impedance of the lumped element can be found as a function of frequency.

Fig. 1(a) shows a generalized, open-ended transmission line with characteristic impedance Z_0 and propagation constant β. It resonates when

$$\frac{n\lambda}{2} = l \tag{1}$$

where n is the order of resonance, and l is the length of the transmission line. The standing wave patterns for the two lowest order modes are shown in Fig. 1(b).

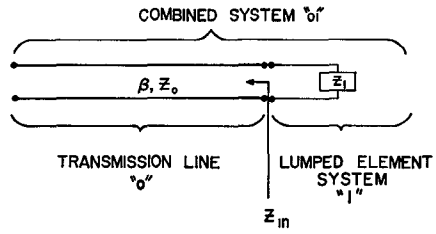

Fig. 2. Resonant system, "01," composed of a transmission line, "0," with an input impedance Z_{in}, and a lumped-element equivalent circuit, "1," with an impedance of Z_1.

A lumped element will perturb the standing-wave pattern when it is connected in shunt between the two conductors where a voltage exists, or when it is connected in series with one connector where a current exists. Fig. 1(c) shows an example of the latter case where the series connection of the capacitor at the midpoint of the line has perturbed mode 1 of Fig. 3(b). Mode 2 is not perturbed since the current is zero at the midpoint and no voltage is developed across the capacitor.

Although the element can be connected anywhere along the transmission line, the two most convenient places are the midpoint and the ends. In general, the series connection of an element at the midpoint affects the odd-order modes, and the shunt connection affects the even-order modes. An end connection of the element affects all modes.

The impedance of the lumped element, expressed here in terms of reactance and Q values, is found from the frequencies and Q's of the transmission line before and after the insertion of the lumped element. Fig. 2 shows a transmission line "0," open circuited at one end, and connected to a lumped element "1," at the other. The combined system "01" resonates when

$$X_1 = Z_0 \cot \theta \tag{2}$$

where X_1 is reactive part of Z_1, and θ is the electrical length of the transmission line. From (16) in the Appendix,

$$\theta = \frac{f}{f_n} n\pi \tag{3}$$

where f is the frequency of resonance of system "01," and f_n is the nth order resonance frequency of the transmission line when both ends are open circuited. Thus the reactance of the lumped element is determined from the two frequencies of resonance.

The Q values for the separate parts of the resonant system "01" add according to their weighted reciprocals as derived in the Appendix (23)

$$\frac{U_{01}}{Q_{01}} = \frac{U_0}{Q_0} + \frac{U_1}{Q_1}. \tag{4}$$

The weighting factors U_{01}, U_0, and U_1 are the stored energies of the combined system, transmission line, and

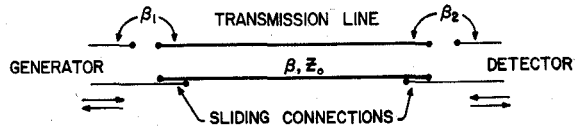

Fig. 3. Schematic of a transmission line showing adjustable coupling to the generator and detector. β_1 and β_2 are coupling coefficients.

lumped element, respectively, and are calculated from the values of the lumped element and electrical length of the line. For example, if the lumped element is an inductor, the definitions of the stored energies given in the Appendix lead to

$$U_0 = \frac{1}{2}\frac{L_0}{\beta}\int_0^{\theta}(I_0 \sin(\beta x))^2 d(\beta x) \tag{5}$$

$$U_1 = \frac{1}{2}L(I_0 \sin\theta)^2 \tag{6}$$

and

$$U_{01} = U_0 + U_1 \tag{7}$$

where L_0 is the inductance per unit length of the line, and L is the inductance of the inductor.

Q_{01} is the measured Q of the system "01," and Q_0 is the Q of the transmission line interpolated to the resonant frequency of the combined system. Thus, with the known values of stored energy, Q_1 can be calculated.

The accuracy of this measurement technique increases as the ratio U_1/Q_1 of (4) becomes larger compared to U_0/Q_0. Thus, for the best accuracy, both the unmodified Q of the transmission line Q_0, and the ratio of energy stored in the lumped element to that of the line U_1/U_0, should be as large as possible. U_1/U_0 is dependent on the Z_0 of the line.

The resonant frequencies and Q's of the transmission line can be measured by transmission or reflection methods as discussed in Ginzton [8]. Fig. 3 shows one method of coupling the generator and detector to the transmission line for transmission measurements. The coupling coefficients β_1 and β_2 are adjusted by moving the end connectors back and forth. When both coupling coefficients are equal[1] and the transmitted power is 40 dB down from the incident power, the measured Q is within 1 percent of the unloaded Q of the transmission line. Rather than being variable, the end couplers can be fixed; in this case, β_1 and β_2 may have to be measured to find the unloaded Q. The transmission method is the least complicated and can be the most accurate.

The *reflection* method of measuring Q has the advantage of requiring only a one-port connection of the generator and the detector. Consequently, there is a greater degree of freedom in the construction of the transmission line and in the connection of the lumped element.

[1] For a detector capable of measuring phase, the condition of $\beta_1=\beta_2$ can be achieved by moving the transmission line back and forth between fixed couplers until the phase is an extremum.

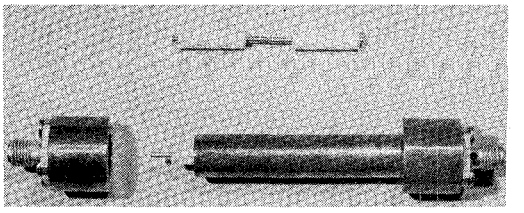

Fig. 4. Resonator used for the Q measurement of capacitors.

Reflection methods have the disadvantage that the determination of Q depends upon the value of the coupling coefficient, which is hard to determine accurately at frequencies in the S-band range and above.[2]

Both coaxial and microstrip lines are suitable for use as transmission-line resonators. Coaxial lines have the advantages of high Q (400 at 1 GHz), negligible dispersion, and low radiation. Microstrip lines have the advantage of open construction, and thus are more accessible for the connection of the lumped element. However, their disadvantages of lower Q (250 at 1 GHz) dispersion and radiation make them less desirable than coaxial lines for lumped-element measurements above 6 GHz.

III. Test Jigs and Measurement Techniques

Examples of coaxial-line resonators used for the measurement of lumped elements are shown in Figs. 4, 5, 7, and 8. The characteristic impedance of the lines is 50 Ω, which results in reasonable U_1/U_0 values for capacitances of about 1 pF and inductances of about 1 nH.

Fig. 4 shows the coaxial transmission line that is used for measuring capacitors.[3] Its center conductor is a 50-mil diameter gold-plated rod, which is insulated from the 162-mil (ID) outer copper conductor by Teflon sleeves that cover its entire length. Two copper sleeves with attached omni spectra miniature (OSM) connectors are used to make sliding electrical connections with the outer conductor. In a manner similar to that shown in Fig. 3, they provide adjustable coupling to the Q-measurement instruments.

The center conductor is severed electrically in the middle to allow for the series connection of a capacitor as shown in the close-up views of Fig. 5. The top view is of a gold-plated quartz rod, with about 10 mils of the plating removed in the middle. A unit of four 0.4-pF capacitors is shown "waxed down" to the conductor, with one of the capacitors bonded between the two halves of the conductor. The lower view shows two gold-plated copper rods joined with a polyethylene dowel with about a 5- to 10-mils spacing between them. One of

[2] A reflection method for determining Q from the frequencies of resonance and extrema in phase (see Ginzton's Eqs. 9.82 and 9.20 [8]) minimizes the dependency of Q on the coupling coefficients. While still more time consuming than the transmission method, it has proven to be equally accurate.

[3] This configuration was originally devised by Hughes, Napoli, and Reichert of RCA Laboratories to measure the resistance of Schottky-barrier diodes [9].

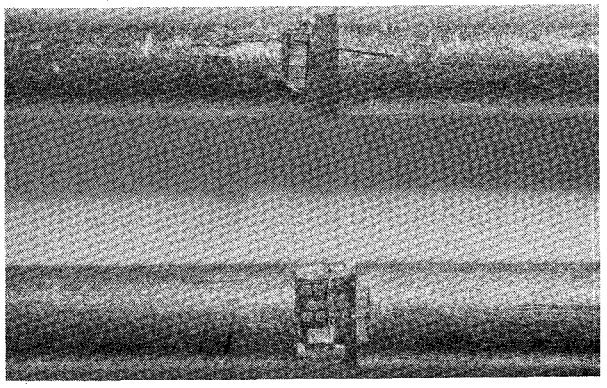

Fig. 5. Enlarged view of the center conductor of the coaxial resonator of Fig. 4 showing the capacitor placement and bonding.

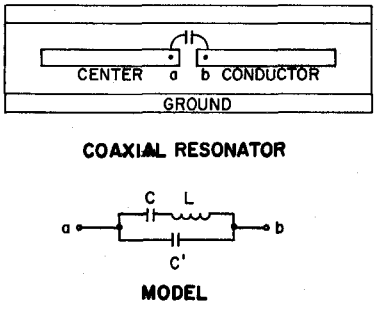

Fig. 6. Equivalent circuit for the capacitor bonded to the coaxial resonator of Fig. 4.

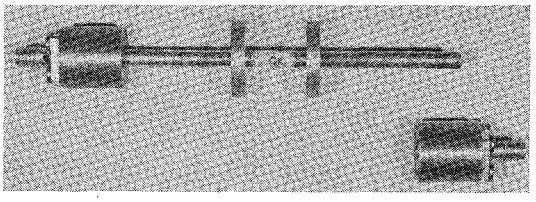

Fig. 7. Coaxial resonator used for the Q measurements of inductors.

the four 0.4-pF capacitors is shown bonded between the two halves. The bond wires are as short as possible to minimize their series resistance. The gap in the rod and the size of the capacitor are kept much smaller than a half wavelength to allow a lumped-element equivalent-model analysis.

Fig. 6 is a drawing of the transmission line with the capacitor attached, and the equivalent-circuit model that results. C' is the capacitance of the gap between the two center conductors, L is the inductance of the bond wire, and C is the capacitance of the capacitor.

The coaxial transmission line used for the measurement of inductors is shown in Fig. 7. It is a 3-in length of commercially available semirigid cable with a 36-mil diameter inner conductor. As with the previous line, the copper sleeves at either end (with OSM connector attached) provide adjustable coupling to the Q-measurement instruments.

Lumped-element inductors cannot be inserted into the coaxial line without causing problems of mutual inductance and standing wave/inductor interactions.

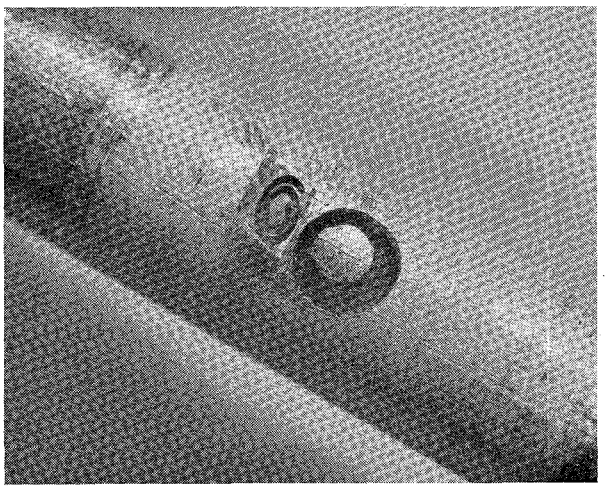

Fig. 8. Close-up view of the resonator in Fig. 7, showing the inductor placement and bonding.

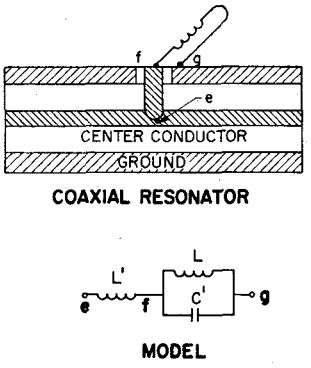

Fig. 9. The equivalent circuit for the inductor bonded to the resonator of Fig. 7.

Consequently, they are mounted outside the coaxial line and are connected in shunt between the outer and inner conductors. Access to the inner conductor is provided by a "pin" inserted through a hole in the outer conductor. Fig. 8 shows a close-up view of a 2-turn inductor connected between the outer conductor and the pin. The plane of the inductor is at right angles to the outer conductor to reduce the mutual coupling.

The brass disks shown in Fig. 7 suppress radiation and wave propagation down the outside of the line. For a disk-to-inductor spacing of less than $\lambda/8$, the effects of these losses are negligible.

Fig. 9 shows the inductor connected to the coaxial line and the resulting equivalent-circuit model. L' and C' are the inductance of the pin and the capacitance between the pin and outer conductor, respectively. L is the inductance of the inductor and bond wire. For spiral- or multi-turn inductors, there is an interturn capacitance; and L should be replaced by a bond-wire inductance in series with a distributed LC combination for the inductor. To the first approximation, the LC combination can be represented by a lumped parallel LC circuit.

The extraneous capacitors and inductors introduced with the connection of the lumped element must be

TABLE I

SAMPLE DATA AND RESULTS FOR THE MEASUREMENT OF A LUMPED-ELEMENT CAPACITOR

f (GHz)	f_0 (GHz)	C (pF)	Q	Q_0	Q_c
1.39419	1.77188	0.75	300	420	620
6.23909	7.10061	0.71	428	770	311

characterized in order to determine the reactance and Q of the lumped element. This is accomplished by making successive measurements—beginning with the unmodified transmission line, making one change at a time and ending with the connection of the lumped element. For example, in Fig. 6 C' and its Q are determined before the capacitor is bonded into place. The inductance L and the Q of the bond wire are determined with the capacitor bonded into place, but short-circuited. Finally, C and its Q are determined with the capacitor open-circuited.

Whenever two elements cannot be physically separated, such as L' and C' of Fig. 9 (without the inductor L), their L and C values are determined from straight-line plots of functions of ω and impedance versus ω^2 (for example, $-jZ\omega = \omega^2 L' - 1/C'$).

Table I shows two sets of sample data and results for the measurement of a lumped-element capacitor connected as shown in Fig. 6. The data are the resonance frequencies and Q values of the transmission line before the line is modified (f_0, Q_0) and after the capacitor is connected (f, Q). The capacitance C is calculated from f and f_0, knowing the values of C' and L of Fig. 6 ($C' = 0.11$ pF, $L = 0.80$ nH). The Q of the capacitor Q_C is calculated from Q and Q_0, knowing C', L, C, and the Q values of C' and L. Q_0 given in Table I is interpolated to the frequency f as discussed in the Appendix.

IV. RESULTS AND DISCUSSION

Using the coaxial transmission-line resonators and the methods discussed in the previous section, lumped-element capacitors from 0.4 to 3.6 pF, and inductors from 1.0 to 4.3 nH in value have been measured at frequencies from 1 to 12 GHz. The results of the measurements are given below.

A. Capacitors

Fig. 10 shows Q versus frequency data for three capacitors and for Q_0, the Q of the unmodified transmission line. The 0.9- and 3.6-pF capacitors have highly densified, low-etch-rate dielectrics,[4] and both capacitors have about equal series resistances. From the Q-versus-frequency curves, their Q values vary nearly as $f^{-3/2}$, and are inversely proportional to the capacitance. The 0.75-pF capacitor has a less-densified, higher etch-rate dielectric. The resistive effects of the bond wire are "subtracted out" from the over-all Q of the capacitor so

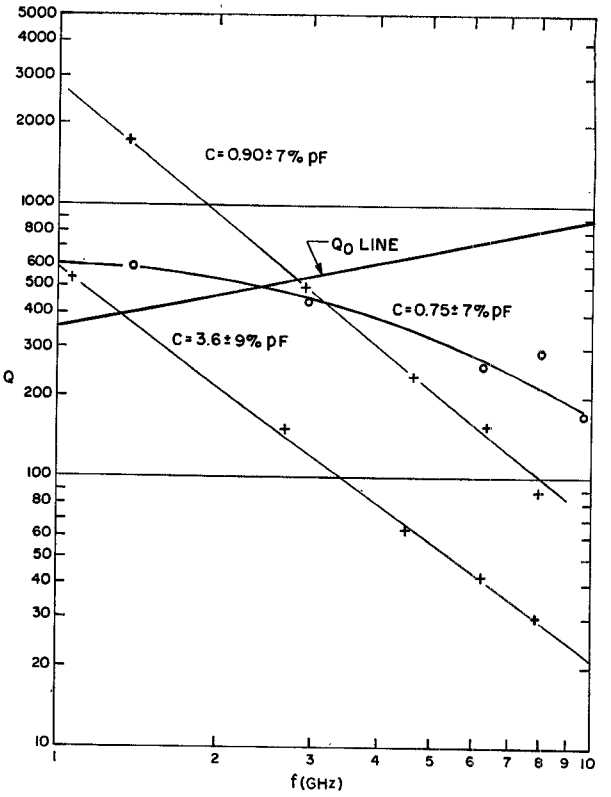

Fig. 10. Q versus frequency for three capacitors and for the unperturbed resonant system (Q_0 line). The 0.75-pF capacitor (corrected for bond wire) shows the effect of dielectric loss.

that the Q values shown in Fig. 10 are due to the capacitor losses only.[5] The Q-versus-frequency curve of this capacitor is almost flat at low frequencies. Similar curves have been obtained for several 0.4-pF capacitors. The capacitance values for all the capacitors are constant to within ± 10 percent through 12 GHz.

It is expected that the losses of a capacitor result from two sources: the dielectric material and the metal conductors. Correspondingly, the Q of the capacitor can be divided into two terms [6]. The equation for the Q of a capacitor with conductor loss only is

$$Q_c = \frac{3W}{2R_s\omega Cl} \tag{8}$$

where C is the capacitance, R_s is the sheet resistance of the metal plates, W is the width, l the length, and ω is the angular frequency. Q_c varies as $f^{-3/2}$ (since R_s changes with skin depth), and inversely with capacitance. The Q of a capacitor with dielectric loss only, is

$$Q_d = \frac{1}{\tan\delta}. \tag{9}$$

The loss tangent of the material, $\tan\delta$, and therefore Q_d, is approximately constant with frequency. The Q of

[4] Generally, a highly densified SiO_2 dielectric has a low etch rate and a low loss.

[5] The other two capacitors were soldered upside down to the center conductor, and no attempt was made to substract the resistive losses of the solder bonds.

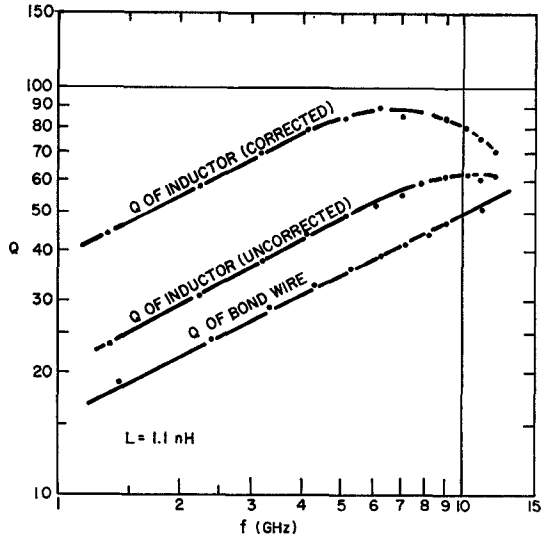

Fig. 11. Q versus frequency for a one-turn 1.1-nH inductor (corrected and uncorrected for bond wire), and for the bond-wire leads.

a capacitor with both kinds of loss is

$$\frac{1}{Q} = \frac{1}{Q_c} + \frac{1}{Q_d}. \tag{10}$$

Fitting (10) to the data gives an estimate of the dielectric and conductor Q values of the capacitor. The straight lines of the 0.9- and 3.6-pF capacitors, and the inverse variation of Q with capacitance suggest a conductor loss only. For the 0.9-pF capacitor this gives an estimate for Q_d of $Q_d > 5000$ (since for $Q_d \leq 3\ Q_c$, the effect of a dielectric Q is noticeable). From the less densified 0.75-pF capacitor, estimates of $Q_d = 600$ and $Q_c = 7200$ at 1 GHz are obtained. Similar results have been obtained from the three 0.4-pF capacitors.

From the estimates of Q_c, a lower limit to the conductor Q of square copper capacitors is,

$$Q_c \geq \frac{5400}{f^{3/2}(\text{GHz})C(\text{pF})}. \tag{11}$$

The difference between the experimentally determined constant 5400 and the theoretically expected value of 29 000 based on the bulk resistivity of copper is not fully explained, although limitations on the exact determination of the constant, the roughness of the surface, and the quality of the evaporated films are important factors.

B. Inductors

Fig. 11 shows Q-versus-frequency curves for a single-turn inductor with and without the resistance of the bond wire (corrected and uncorrected, respectively), and for the bond wire itself. The Q for the inductor (corrected) increases as $f^{1/2}$ at frequencies below 4 GHz as expected from the theoretical expression,

$$Q = \frac{\omega L}{R} \tag{12}$$

where L is the inductance and R is the series resistance. The value for Q at 2 GHz corresponds to that predicted from theory [1]. Above 4 GHz the Q falls off from its $f^{1/2}$ variation and eventually decreases. The reason for the fall-off and decrease is not known although current crowding and radiation are possible explanations. All inductors measured exhibit the same fall-off at the higher frequencies. The measured inductance of 1.1 nH, which is constant to within ± 5 percent through 12 GHz, is equal to that predicted from theory [1] [10].

Multi-turn or spiral inductors (see Fig. 8) are found to have higher Q and inductance values per square area than single-turn inductors, although the Q values are less than predicted (from [1]) and the Q-versus-frequency plots fall off at lower frequencies. The measured and theoretical values of inductance are nearly the same.

A spiral-turn inductor has an associated interturn capacitance that resonates with the inductance. The self-resonance frequencies of these inductors is much lower than those for a single-turn inductor. For example, a two-turn, 2.9-nH inductor can have a self-resonance frequency of 8 to 10 GHz, whereas a single-turn 1.1-nH inductor shows no distributed effects up to 12 GHz.

V. Conclusions

A technique for the measurement of reactance and Q values of small, microwave lumped-element inductors and capacitors has been presented. It extends the capability for lumped-element measurements up to 12 GHz by making use of the accurately measured frequencies and Q's of resonant coaxial lines. Using the technique, Q values as high as 1700 at 1.4 GHz and 100 at 12 GHz have been measured. The results of measurements on capacitors and inductors show that lumped elements can be fabricated with low loss and constant L and C values through X band.

Appendix

Presented below are the derivations of the equations for calculating the reactance and Q of a lumped element from the measured resonance frequency and Q data. It is assumed, in all cases, that the reactances are much larger than the resistances so that the two can be treated separately.

A. Resonance Condition

Fig. 2 shows an open-circuited transmission line "0," with an input impedance Z_{in}, connected to a lumped-element circuit "1," with impedance Z_1. Neglecting the resistances, the combined system resonates when the reactive part at Z_1 is equal to the complex conjugate of Z_{in}, or

$$jX_1 = jZ_0 \cot \theta \tag{13}$$

where

$$\theta = \frac{2\pi f l}{v} \tag{14}$$

and f, l, and v are the frequency of resonance, the length, and the velocity of wave propagation of the transmission line, respectively, and X_1 is the reactance of the lumped-element circuit.

Without the lumped elements attached, the transmission line resonates when

$$\theta = \frac{2\pi f_n l}{v} = n\pi \tag{15}$$

where f_n is the nth-order resonance frequency. Substituting (15) into (14) gives θ in terms of two resonance frequencies,

$$\theta = \frac{f}{f_n} n\pi. \tag{16}$$

Combining (16) and (13) results in the final equation for the resonance condition,

$$X_1 = Z_0 \cot\left(\frac{f}{f_n} n\pi\right). \tag{17}$$

If the lumped-element circuit is connected in the middle of the transmission line, f is replaced by $f/2$; also, for a series connection, Z_0 is replaced by $2Z_0$, and for a shunt connection Z_0 is replaced by $Z_0/2$.

The reactance X_1 of the lumped-element circuit is determined from f, f_n, n, and Z_0. As mentioned in Section III, when Z_1 is due to more than one element, the reactance of each element is determined by successive measurements.

B. The Q Equation

Reference to Fig. 2 shows that the total power loss of the resonant system "01" is equal to the power losses of the transmission line "0," and the lumped-element circuit "1" (which consists of i elements):

$$P_{01} = P_0 + \sum P_{1i}. \tag{18}$$

The quality factor Q of a resonant system is related to the power loss P and the stored energy U of the system by,

$$Q = \frac{\omega U}{P}. \tag{19}$$

Thus for the combined system "01,"

$$Q_{01} = \frac{\omega U_{01}}{P_{01}}. \tag{20}$$

For the ith lumped element of circuit 1, Q is defined as,

$$Q_{1i} = \frac{\omega U_{1i}}{P_{1i}} \tag{21}$$

where U_{1i} is the *maximum* energy stored in the element. This definition is equivalent to the conventional definitions of the Q for lumped elements.

A Q variable, Q_0 is defined for the transmission line "0," as,

$$Q_0 = \frac{\omega U_0}{P_0} \tag{22}$$

where U_0 is the energy stored in the transmission line when the current is maximum. Q_0 corresponds to the measured Q when the transmission line is self-resonant; and for transmission lines with a series loss only, such as the coaxial lines described in Section III, Q_0 is a "straight-line" function of frequency when plotted on log–log paper.

Substituting (20), (21), and (22) into (18) gives:

$$\frac{U_{01}}{Q_{01}} = \frac{U_0}{Q_0} + \sum \frac{U_{1i}}{Q_{1i}}. \tag{23}$$

This corresponds to (4) in the text, where only one lumped element is considered. The Q of the jth element Q_{1j} can be found by rewriting (23) as,

$$\frac{1}{Q_{1j}} = \frac{1}{U_{1j}}\left(\frac{U_{01}}{Q_{01}} - \frac{U_0}{Q_0} - \sum{}' \frac{U_{1i}}{Q_{1i}}\right) \tag{24}$$

where $\sum'$ is the sum for all i, $i \neq j$.

The stored energy for the transmission line is

$$U_0 = \frac{1}{2}\frac{L_0}{\beta}\int_0^\theta (I_0 \sin(\beta x))^2 d(\beta x) \tag{25}$$

$$= \frac{1}{8}\frac{Z_0}{\omega} I_0^2 (2\theta - \sin 2\theta) \tag{26}$$

where θ is defined in (16). The maximum energy stored in each of the lumped elements U_{1i} is calculated from a knowledge of the current going into the entire lumped element system, the current in the transmission line,

$$I = I_0 \sin\theta \tag{27}$$

the particular circuit model of Z_1, and the values of the lumped elements. The total stored energy can be calculated for the maximum current condition, where

$$U_{01} = U_0 + \sum{}'' U_{1k} \tag{28}$$

where $\sum''$ is the summation of U_{1k} for inductors only $(k \neq j)$.

Equations (26), (27), and (28) apply for the case where the lumped element is connected in the middle of the transmission line when the substitutions following (17) are made.

Q_0 is the Q of the transmission line interpolated from the measured Q versus frequency data to the resonance frequency of the combined system "01," and Q_{01} is the measured Q of system "01." The Q_{1i} are the Q's of the "i" lumped elements, which are determined by separate measurements.

Acknowledgment

The author wishes to thank M. Caulton for his direction and helpful suggestions, and B. Hershenov, L. S. Napoli, and L. S. Nergaard for their valuable discus-

sions. He also wishes to thank R. Chamberlain, W. Dimitruk, R. Goodrich, N. Klein, A. Young, and L. Zappulla, all of whom were associated with the fabrication of the lumped elements, construction of the resonators, and uniting of the two.

References

[1] M. Caulton, S. P. Knight, and D. A. Daly, "Hybrid integrated lumped-element microwave amplifiers," *IEEE Trans. Electron Devices (Special Issue on Microwave Integrated Circuits)*, vol. ED-15, pp. 459–466, July 1968.
[2] M. Caulton *et al.*, "UHF film integrated circuits," Contract DAAB07-68-C-0296, Tech. Reps. ECOM-0296-1-6 (1st through 6th Quart. Reps.).
[3] M. Caulton and W. E. Poole, "Designing lumped elements into microwave amplifiers," *Electronics*, Apr. 14, 1969.
[4] M. Caulton, B. Hershenov, S. P. Knight, and R. E. DeBrecht, "Status of lumped elements in microwave integrated circuits—present and future," *IEEE Trans. Microwave Theory Tech. (Special Issue on Microwave Integrated Circuits)*, vol. MTT-19, pp. 588–599, July 1971.
[5] G. D. Alley, "Interdigital capacitors and their application to lumped-element microwave integrated circuits," to be published.
[6] M. Caulton, "The lumped element approach to microwave integrated circuits," *Microwave J.*, May 1970.
[7] D. A. Daly, S. P. Knight, M. Caulton, and R. Ekholdt, "Lumped elements in microwave integrated circuits," *IEEE Trans. Microwave Theory Tech.*, vol. MTT-15, pp. 713–721, Dec. 1967.
[8] E. L. Ginzton, *Microwave Measurements*. New York: McGraw-Hill, 1957, ch. 9.
[9] J. J. Hughes, L. S. Napoli, and W. F. Reichert, "Novel technique for measuring the Q factor of thin-film lumped-elements at microwave frequencies," *Electron. Lett.*, vol. 5, no. 21, p. 535, Oct. 1969.
[10] F. W. Grover, *Inductance Calculations, Working Formulas and Tables*. New York: Van Nostrand, 1946.

Digitized Antenna Measurements

JAKOB DIJK, CORSTIAAN KRAMER, EDUARD J. MAANDERS, SENIOR MEMBER, IEEE, AND ADRIAAN C. A. VAN DER VORST

***Abstract*—A low-cost automated measuring method is presented to determine the directive gain and relative phase of microwave antenna feed systems in digital form. Using large existing computer facilities, the output data may be used as input data to compute secondary patterns of arbitrary reflector antennas. The use of stepping motors is a key for cheaper and easier operations.**

Introduction

IN MODERN ANTENNA engineering, especially for long-range radar, radio astronomy, satellite communications ground stations, or multibeam antenna systems for satellites, it is very important to know the antenna pattern as regards amplitude and phase and its polarization in all directions. Mostly, the current distribution method is used to calculate the entire radiation pattern of bodies of revolution.

Silver [1, p. 420] has developed a number of formulas enabling one to calculate the secondary pattern of a paraboloid with the source at the focus, while Rusch [2], [3] has demonstrated that the same technique may be used for a hyperboloid or ellipsoid. It is not the purpose of this paper to go into details with regard to the complicated equations used for calculation, but it appears that in all equations the directive gain $D(\theta, \phi)$ [4] and its relative phase pattern of the primary feed play an important role. Other applications, such as designing double reflector systems [5] with high efficiency, require detailed information with regard to the feed pattern.

Manuscript received March 11, 1971; revised August 30, 1971.
The authors are with the Eindhoven University of Technology, Eindhoven, The Netherlands.

Sometimes the performance of an antenna system may be predicted by using "theoretical" feeds, the class of circular symmetrical feed patterns defined by

$$D(\theta) = 2(n + 1) \cos^n \theta$$

having become very popular.

The Eindhoven University of Technology, Eindhoven, The Netherlands, now possesses several computer programs to calculate secondary patterns of paraboloids, hyperboloids, and ellipsoids excitated by this theoretical feed pattern at their focuses. Moreover, programs are available to design double reflector systems with the same "theoretical" feed system. However, in most cases one wants to know the performance of an antenna with a practical feed system. In the past, antenna patterns have been plotted on paper and presented as graphs, the field strength, power density, and phase being represented relative to a reference value, mostly the peak of the beam.

If the directivity of such an antenna is required, an accurately calibrated gain standard has to be used. These measurements are not only time consuming but also unsuitable for use in the computer programs previously discussed. This paper presents some inexpensive digital techniques in antenna measurements both for amplitude and phase. Digital techniques are particularly useful in applications involving large quantities of data, such as antenna measurements. The results, in the form of punched paper tape are available immediately after the measurements, which permits direct entry into a computer (see computer programs [6]).